Extrinsic Signatures Embedding and Detection for Information Hiding and Secure Printing in Electrophotography

Pei-Ju Chiang[2], Gazi N. Ali[1], Aravind K. Mikkilineni[1],
Edward J. Delp[1], Jan P. Allebach[1], and George T.-C. Chiu[2]
[1]School of Electrical and Computer Engineering
[2]School of Mechanical Engineering
Purdue University, West Lafayette, IN 47907 USA
pchiang@purdue.edu

***Abstract*—Printer identification based on printed documents can provide forensic information to protect copyright and verify authenticity. In addition to intrinsic features (intrinsic signatures) of the printer, modulating the printing process to embed specific features (extrinsic signatures) will further extend the encoding capacity and accuracy. One of the key issues with embedding extrinsic signature is the information should not be detectable by the human observer, but needs to be detectable by a suitable detection algorithm. In this paper, we will discuss the methods used to develop the amplitude threshold and frequency constraints for embedding extrinsic signature in electrophotography by modulating laser intensity.**

I. INTRODUCTION

Printed material is a direct accessory to many criminal and terrorist acts. Examples include forgery or alteration of documents used for purposes of identity, security, or recording transactions. In addition, printed material may be used in the course of conducting illicit or terrorist activities. Examples include instruction manuals, team rosters, meeting notes, and correspondence. In both cases, the ability to identify the device or type of device used to print the material in question would provide a valuable aid for law enforcement and intelligence agencies.

We are developing two strategies for printer identification [1]. The first one is passive. It involves tracing the intrinsic features in the printed output that are characteristic of the particular printer, model, or manufacturer's products. We called this the intrinsic signature. The second strategy is active. This involves modulating the process parameters in the printer mechanism to encode identification information such as the printer's serial number and date of printing. We called this the extrinsic signature. Depending on the purpose of embedding, the signature of a printer sometimes needs to be fragile where any deviation from the legitimate process will destroy the signature or it needs to be robust where the signature will be difficult to be altered or removed. The advantages of exploiting modulating the printing process as potential signature lie in the high barrier of entry for possible attack scenarios [2].

Banding is one of the most noticeable image artifacts for electrophotographic (EP) printers, e.g. laser printer. It manifests as contrast variations (periodic or random light and dark bands) on a printed page and is especially visible in the mid-tone area. As an image artifact, banding has received significant attention in recent years. Many approaches have been shown to be effective in reducing banding by modulating EP process parameters such as laser intensity or timing [3] and motor speed [4] to compensate for process disturbances such as gearing noise. These methods can also be used to inject properly designed banding signatures.

Due to its origin within the EP process, banding can be viewed as an intrinsic signature of the specific printer. Modulating the EP process to generate banding signals that are below the human visual threshold but can be detected by effective detection approach can further extend the signature capacity and capability. The ability to precisely control the EP process and modulate unperceivable but detectable banding is essential.

One of the key issues with embedding extrinsic signature is the information should not be detectable by the human observer but needs to be detectable by suitable detection algorithms [5]-[9]. To accomplish this, we will exploit the band-pass characteristics of the human visual system to contrast variations, where the human visual system has relative low sensitivity for high spatial frequency contrast variations. Among the process modulating methods [3,4], motor control will have difficulty to affect the EP process at high spatial frequencies due to the inherent electro-mechanical limitations. Modulating various laser parameters to affect exposure is common practice in EP process control. The mapping between the modulation parameter and the resulting contrast variation need to be determined to ensure that the extrinsic banding signature is below the human detection threshold.

In our previous work [10, 11], we have reported techniques of modulating the exposure of the EP process through laser intensity modulation. Due to the nonlinear EP process, a sinusoidal modulation of the laser intensity will result in contrast variation composed of multiple frequency components. The nonlinearity of the EP process will complicate the process of finding the modulating threshold to stay below the human contrast sensitivity threshold.

In this paper we will discuss the process of developing the modulating threshold based on physical and empirical models of the EP process as well as the associated detection algorithm. Experimental results using an off-the-shelf office laser printer will be presented to verify the effectiveness of the proposed technique.

The remaining of the paper is organized as follows. The EP process and its modeling are presented in the next section followed by the discussion of the approaches used to develop the modulating threshold. The analysis of frequencies contents in the printout will be presented in the forth section followed by experimental validation. Summary and conclusions are given in the last section.

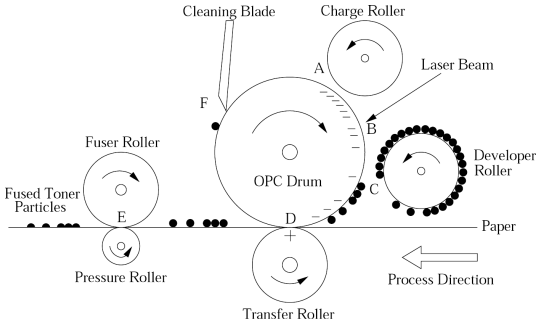

Figure 1 Electrophotographic process: cross-section of a typical laser printer (A) charging, (B) exposure, (C) development,(D) transferring, (E) fusing, and (F) cleaning.

II. Electrophotographic Process and Laser Intensity Modulation

The electrophotographic process [12] can be described in six main steps, namely charging, exposure, development, transferring, fusing, and cleaning. Figure 1 shows these steps on the cross-section of a laser printer. First, the charger roller uniformly charges the organic photoconductor (OPC) drum surface to a constant negative voltage. In the exposure step, a laser beam is scanned across the OPC and is turned on to discharge the OPC surface at appropriate locations. These discharged locations then attract the negatively charged toner particles in the development step. After development, the transfer roller applies a positive charge to the paper. This positive charge creates a force pulling the negatively charged toner particles to the paper. Next the paper passes between a heated fuser roller and a pressure roller, which together melt the toner and fuse them onto the paper. The non-transferred toner particles on the OPC drum are removed with the help of a blade or a brush during the cleaning step.

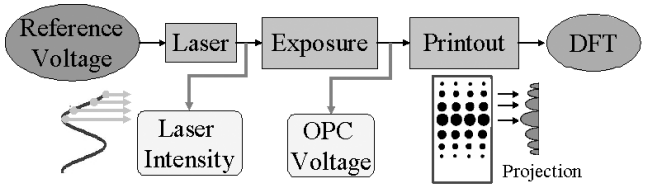

Figure 2 Process block diagram for embedding and detecting extrinsic banding signature using laser intensity modulation.

Modulating the laser intensity effectively modulates the exposure (discharge) process on the surface of the OPC drum and changes the size of the dots (dot gain) form by the toner particles. The changes in dot gain result in changes in effective contrast as viewed by the human observer. Introducing sinusoidal modulation in the laser intensity will result in harmonic contrast modulation of the printed image that can be detected after the image is scanned. This is the fundamental process for embedding extrinsic signatures into a document. Figure 2 shows basic process block diagram of embedding banding signals by modulating the laser intensity in an EP process. One should note that to maintain process stability, there is only a limit range of the laser intensity that can be used for signature embedding. Figure 3 illustrates the process to embed and detect extrinsic banding signals used in this study. After embedding banding signal into a printed image, the image will be scanned and the resulting 2D absorptance data is projected onto the process direction to form a 1D absorptance signal. DFT will be performed on the projected absorptance signal to extract the frequency contents.

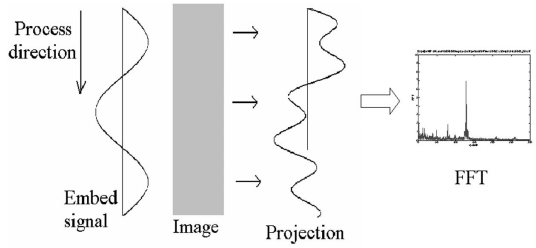

Figure 3 Embedding and detecting extrinsic banding signal

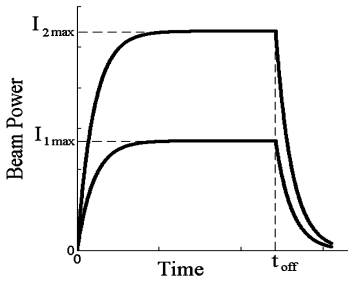

Figure 4 Temporal response of a laser pulse

A. Laser Intensity Modulation

To take the advantage of the effect of laser intensity on the EP process, a combined physical and experimental EP process with laser intensity as input and dot gain contrast as output need to be developed. The intensity profile of the laser is modeled as a 2-D Gaussian envelope [13,14] given by

$$I(x,y,t) = I_0(t)\mathrm{e}^{(-y^2/2\alpha^2 - x^2/2\beta^2)} \quad [W/m^2], \qquad (1)$$

where $I_0(t)$ represents the power amplitude of the laser, and β and α are the beam widths in the scan x, and process y, directions, respectively. Assume the laser is switched on at time 0 and off at time t_{off} and the rise and fall transition are modeled as an exponential function, see Figure 4. The laser intensity profile can be expressed as

$$I_0(t) = \begin{cases} 0, & t < 0, \\ I_{\max}(1 - \mathrm{e}^{-\frac{t}{t_r}}), & 0 \le t \le t_{off}, \\ I_{\max}(1 - \mathrm{e}^{-\frac{t_{off}}{t_r}}) \cdot e^{\frac{-(t-t_{off})}{t_f}}, & t > t_{off}, \end{cases} \qquad (2)$$

Let the nominal values of the printed pixel width in the scan direction and process direction be X and Y, respectively. Assume the laser beam translates along the scan direction x, at a velocity v, which is extremely high compared with the motion of the photoconductor surface. Then the exposure energy at any arbitrary point (x, y) due to the pixel [m, n]

being turned on is found by integrating Eq. (2) with respect to time, i.e.

$$E_{mn}(x,y) = \int I_0(t)\exp(-\frac{(y-y_n)^2}{2\alpha^2} - \frac{(x-(x_m - X/2) - vt)^2}{2\beta^2})dt \quad [J/m^2]. \quad (3)$$

Since the exposure of each printed pixel is additive, the overall exposure at any given point on the OPC surface is the sum of exposures contributed from each neighboring pixel in the halftone, i.e.

$$E(x,y) = \sum_{m,n} E_{mn}(x,y). \quad (4)$$

To control the exposure, one can either adjust the input voltage to the laser (amplitude modulation), or adjust the duration of the laser pulses (pulse width modulation or PWM) [3]. Both methods control $I_0(t)$, i.e. the power amplitude of the laser beam. In this study, amplitude modulation is used to control exposure. As shown in Figure 4, when $I_{\max}$ increases, the beam power $I_0(t)$ and the total exposure energy also increases. Through modulating the laser power amplitude, which is linearly propotional to the reference voltage to the laser power control circuit, the exposure energy is adjusted and results in different dot sizes.

Figure 5(a) shows the average dot profile of 16 dots when the input voltage is 1.1, 1.3, 1.5 and 1.7 volt, respectively. Figure 5(b) shows the relationship between the laser intensity reference voltages and dot size. The dot size is determined by counting the number of pixels with an absorptance value greater than 0.1 in one dot cell. As seen in Figure 5, as input voltage increases, the corresponding dot size increases. However, the variation in the EP process results in variations in the corresponding dot sizes.

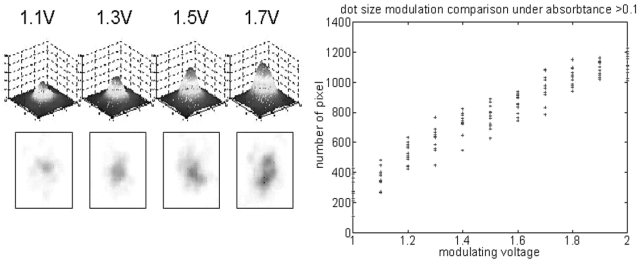

(a) (b)

Figure 5 Dot size and laser intensity modulation

Since bigger dots have more toner and higher absorptance, we can create a periodic signal through arrangement of various sizes of dots. The dot size modulation is synchronized with each scan line in the scan direction along the axial direction of the OPC drum. For a 600 dpi printer, the highest banding frequency that can be created is 300 cycles/in. However, due to the sampling effect of modulating dot size per scan line, several classical signal processing issues will need to be considered such as harmonics and frequency quantization.

III. Laser Modulation Threshold

As discussed in the first section, to embed unperceivable banding signal in printed document, the resulting contrast variation needs to be below the human contrast sensitivity threshold. Since the laser intensity is the actual input signal, it is therefore important to derive the corresponding laser intensity modulation threshold. However, since contrast is a relative measure, the corresponding laser intensity modulation threshold will also depend on the desired tone of the image.

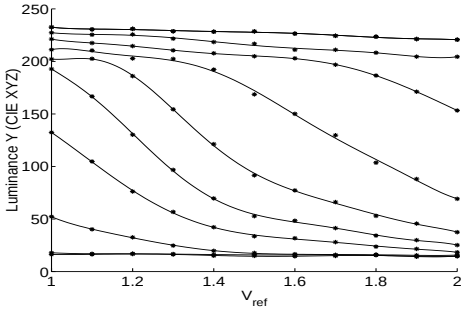

Figure 6 Mapping between reference voltage and luminance of printouts with various default gray values from 10% through 100%

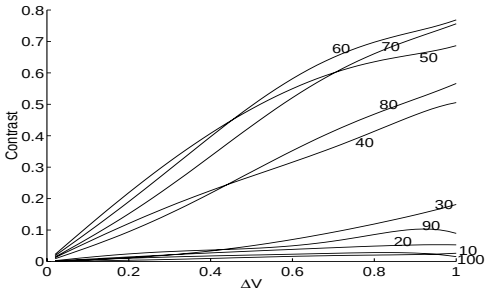

Figure 7 Mapping between ΔV and contrast

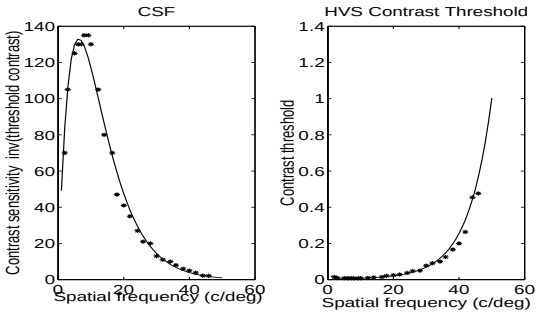

Figure 8 Human contrast sensitivity function (CSF) and the corresponding human visual system (HSV) contrast threshold (2.0 mm pupil with 57 in viewing distance) [16]

To modulate laser intensity, we adjusted the reference voltage input V_{ref} to the laser power control circuit with the following voltage signal:

$$V_{ref} = V_0 + \frac{\Delta V}{2} \cdot \sin(w_0 y), \quad (5)$$

where V_0 is the nominal reference voltage, w_0 is the spatial banding frequency, and ΔV is the peak-to-peak amplitude of the variation to the reference voltage that will result in contrast variation. To obtain the mapping between laser intensity modulation ΔV and the resulting contrast variation, test pages with 10 gray levels from 10% to 100% in 10% increments are generated using the printers default halftone. The test pages are printed with various different intensity modulations and then scanned with a calibrated scanner and the associated contrasts are calculated from the scanned data. Since Michelson contrast C [15] is often used for periodic test

patterns such as sinusoidal and square gratings, it is used in this study and its definition is as following:

$$C = \frac{Y_{\max} - Y_{\min}}{Y_{\max} + Y_{\min}} , \quad (6)$$

where Y_{max} and Y_{min} are the maximum and minimum luminance in CIE XYZ coordinates, respectively.

Figure 6 shows the measured mapping between the reference voltage and the measured luminance of printed test pages. Generally, the luminance decreases when the reference voltage increases. We can model this nonlinear relationship by a third order polynomial

$$Y = a_3 V_{ref}{}^3 + a_2 V_{ref}{}^2 + a_1 V_{ref} + a_0 \quad (7)$$

Substitute V_{ref} in Eq. (5) into the above equation we have

$$\begin{aligned} Y = & -1/4 \cdot A_3(\Delta V)^3 \sin(3w_0 y) \\ & -1/2 \cdot A_2(\Delta V)^2 \cos(2w_0 y) \\ & +[3/4 \cdot A_3(\Delta V)^3 + A_1(\Delta V)]\sin(w_0 y) \\ & +1/2 \cdot A_2(\Delta V)^2 + A_0 \end{aligned} , \quad (8)$$

where equations $\sin^3\theta = (3/4)\sin\theta - (1/4)\sin 3\theta$, and $\sin^2\theta = (1/2)(1-\cos 2\theta)$ are used in deriving Eq. (8). By matching coefficients, we can obtain

$$\begin{aligned} A_3 &= a_3/8 \\ A_2 &= (3a_3 V_0 + a_2)/4 \\ A_1 &= (3a_3 V_0{}^2 + 2a_2 V_0 + a_1)/2 \\ A_0 &= a_3 V_0{}^3 + a_2 V_0{}^2 + a_1 V_0 + a_0 \end{aligned} .$$

From Eq. (8), Y_{min} and Y_{max} can be obtained as

$$\begin{aligned} Y_{\min} &= A_3(\Delta V)^3 + A_2(\Delta V)^2 + A_1(\Delta V) + A_0 \\ Y_{\max} &= -A_3(\Delta V)^3 + A_2(\Delta V)^2 - A_1(\Delta V) + A_0 \end{aligned} . \quad (9)$$

Substituting Eq. (9) into Eq. (6), for a given nominal grey value, we can obtain contrast as a function of the laser intensity variation ΔV as

$$C = C(\Delta V) = -[A_3(\Delta V)^3 + A_1(\Delta V)]/[A_2(\Delta V)^2 + A_0] . \quad (10)$$

Based on Eq. (10), Figure 7 shows the contrast as a function of the laser intensity variation in terms of the reference voltage variation.

In order to embed unperceivable banding signatures, a proper intensity modulation ΔV needs to be selected so that the resulting contrast is under the HVS contrast threshold, see Fig. 8. The contrast threshold $C_{TH}(\omega)$ for a given spatial frequency ω can be obtained from Fig 8. Given $C_{TH}(\omega)$, the ΔV threshold $\Delta V_{TH}(\omega)$ as a function of the spatial frequency, can be obtain by $\Delta V_{TH}(\omega) = C^{-1}(C_{TH}(w))$. Figure 9 shows the resulting $\Delta V_{TH}(\omega)$ for different grey levels. As can be seen from Figure 9, the corresponding ΔV_{TH} is too low to be detected by the scanner for a wide range of spatial frequencies. This implies that only limited banding signal can be embedded without affecting the perceived image quality. However, when the spatial frequency is higher than 45 cycles per degree, the ΔV_{TH} is high. This is another indication that higher spatial frequencies are the potential regions for embedding extrinsic banding signatures.

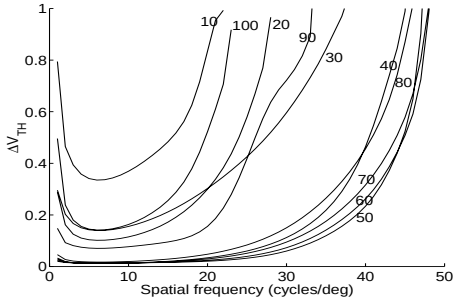

Figure 9 Mapping between the ΔV_{TH} threshold and the spatial frequency for difference desired gray levels

IV. Signature Detection

To detect the embedded banding signatures, the printed document needs to be scanned and the necessary image analysis algorithms can be applied to the scanned digital image. Figure 10 illustrates the procedure from a signal processing and communication point of view. The original intensity modulation can be viewed as the input signal to the transmission channel composed of two sample and filter pairs, the printer (EP process) and the scanner. Both the printer and scanner resample the banding signature at their respective native resolution and filter the signature based on their respective modulation transfer function (MTF). To detect the original signature from the scanned image, several fundamental issues in signal processing need to be addressed.

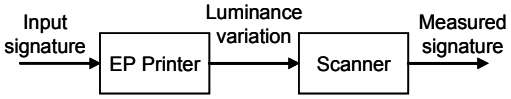

Figure 10 Signature embedding and detection

A. Harmonic frequencies and alias

Given a single frequency sinusoidal intensity modulation, the nonlinear EP process will generate printout that has luminance/reflectance fluctuations at multiple harmonics of the initial frequency. The luminance fluctuation will then be re-sampled by the scanner at its native resolution.

Typical printer MTF has low-pass characteristics with a bandwidth determined by the halftone or screening process. Typically, it will be less than half of the native resolution of the printer. This frequency acts as the upper-bound of the signature. During the scanning process, one needs to carefully select the scanning resolution to avoid the possibility of aliasing. One interesting aspect of the current process is that the low-pass MTF characteristics of the printer and scanner may have the anti-aliasing effect and reduce the impact of aliasing in the process. The validity to this requires further study and is not considered in this paper.

B. Multi-frequency modulation – beating effect

One of the potential methods to increase the capacity of the signature is to include multiple frequencies in the banding signature. However, the impact of such practice has some interesting consequences due to the effect of frequency beating. Recall that when two sinusoidal signals are combined, the resulting signal can be viewed as an amplitude modulated signal with the amplitude determined by the difference of the two frequencies and the carrier signal is

closed to the mean of the two frequencies. If two sinusoidal components are included in the intensity modulation, let the V_{ref} variation contains two frequencies w_1 and w_2. Without loss of generality, V_{ref} can be written as

$$V_{ref} = V_0 + \Delta V / 4 \cdot [\cos(w_1 y) + \cos(w_2 y)] . \quad (11)$$

Substituting Eq. (11) into Eq. (7), the corresponding luminance become

$$\begin{aligned} Y &= a_3 V_{ref}^{\ 3} + a_2 V_{ref}^{\ 2} + a_1 V_{ref} + a_0 \\ &= 1/32 \cdot A_3 (\Delta V)^3 \{9[\cos(w_1 y) + \cos(w_2 y)] \\ &\quad + 3[\cos((2w_1 - w_2) y) + \cos((w_1 - 2w_2) y)] \\ &\quad + [\cos(w_1 y) + \cos(w_2 y)]\} \\ &\quad + 1/8 \cdot A_2 (\Delta V)^2 \{2 + 2\cos((w_1 + w_2) y) \\ &\quad + 2\cos((w_1 - w_2) y) + \cos((2w_1) y) + \cos(2w_2 y)\} \\ &\quad + A_1 (\Delta V)/2 \cdot \{\cos(w_1 y) + \cos(2w_2 y)\} + A_0 \end{aligned} \quad . \quad (12)$$

As can be seen from Eq. (12), eight additional frequency components are present in the luminance. Since for signature embedding, ΔV is typically very small. The luminance can be simplified to

$$\begin{aligned} Y &\approx A_1 (\Delta V)/2 \cdot \{\cos(w_1 y) + \cos(w_2 y)\} + A_0 \\ &= A_1 (\Delta V) \{\cos(\frac{w_1 + w_2}{2} \cdot y) \cdot \cos(\frac{w_1 - w_2}{2} \cdot y)\} + A_0 \end{aligned} , \quad (13)$$

and the corresponding contrast is

$$C = -A_1 \Delta V / A_0 . \quad (14)$$

Equation (13) represents a product of two cosine signals with a beat frequency given by

$$w_b = 2 \cdot (w_1 - w_2)/2 = w_1 - w_2 . \quad (15)$$

The frequency components that will be visible to human is the beat frequency w_b and $(w_1+w_2)/2$, but not the frequencies w_1 and w_2, which will be detected by the DFT analysis. Hence, to embed unperceivable banding in this case, we need to find the ΔV_{TH} corresponding to w_b and $(w_1+w_2)/2$ but not w_1 and w_2.

To demonstrate this phenomenon, a test page was printed with w_1=10, w_2=15 cycles per inch and amplitude ΔV=0.5V. The printout and the DFT analysis are shown in Fig. 11(b) and Fig. 12, respectively. For comparison, the printout with single frequency 5 and 12.5 cycles per inch and amplitude ΔV=0.5V are shown in Fig. 11(a) and 11(c), respectively. We can see that although Fig. 11(b) seems to have frequencies 5 and 12.5 cycles per inch, the DFT, shown in Fig. 12, indicates strong energy at 10 and 15 but not 5 or 12.5 cycles per inch. The little energy at 5 and 25 cycles per inch can be explained by Eq. (12). Note that the frequency at 100 cycles per inch shown in Fig. 12 is the intrinsic signature of the printer resulted from process variation of manufacturing. To embed extrinsic signature, we need to avoid overlapping with the intrinsic signature of the printer, 100 cycles per inch in this case. If we modulate the intensity under the ΔV thresholds, the 5 and 25 cycles/in will disappear from the DFT plot. That is because when the amplitude ΔV is extremely small, the mapping between reference voltage and luminance of printout can be approximately presented as a linear equation. However, ΔV has to be large enough to be detected. The probability of correct detection depends on the signal embedding and detection algorithm [17].

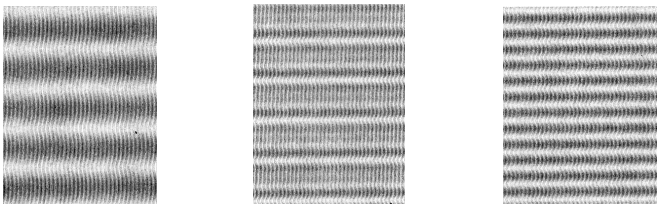

(a) (b) (c)

Figure 11 (a) Printout with modulation of frequency 5 cycles/in and amplitude 0.5 V (b) Printout with modulation of two frequencies 10, 15 cycles/in and amplitude 0.5 V (c) Printout with frequency 12.5 cycles/in, amplitude 0.5 V.

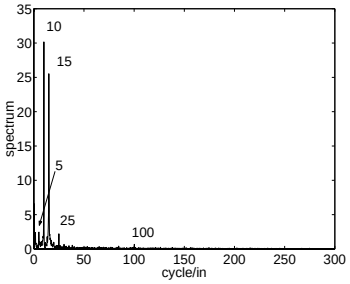

Figure 12 Spectrum of the projected reflectance for Fig. 11(b)

V. Experimental Verification

To demonstrate embedding extrinsic signature into haltone images, a natural image with large regions of smooth mid-tone is selected, see Fig. 13. Figure 14 shows the projected absorptance spectrum of the original printed test image without embedding any banding signature. As can be seen, frequency peaks at 75, 100, and 150 cycles per inch are present. This frequency pattern is the intrinsic signature of the printer that resulted from process manufacturing variation or halftone screens. To embed extrinsic signature, we need to avoid overlapping with the intrinsic signals in the printer. In this example, 90, 110 and 130 cycles per inch banding signals with intensity variation $\Delta V = 0.05$ will be embedded. Figure 15 shows the printed image with embedded signature. It is clear that there is not visible degradation in image quality and the embedded banding signals are not visible. Figure 16 shows the absorptance spectrum of the printed image with signature embedded. The original 75, 100, and 150 cycles per inch intrinsic bands are still present. However, the 90, 110 and 130 bands are also detectable. Note that the 130 cycle per inch peak is very weak. Although the same intensity modulation ΔV is applied, we observe a decrease in the effect. This is attributed to the combined MTF characteristics of the printer and the scanner. More work is needed to compensate for these device characteristics.

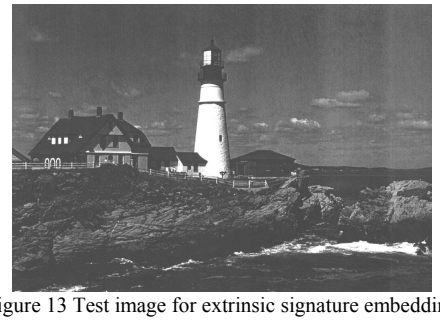

Figure 13 Test image for extrinsic signature embedding

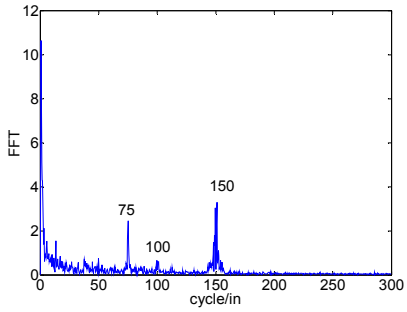

Figure 14 Spectrum of the projected absorptance for the original image.

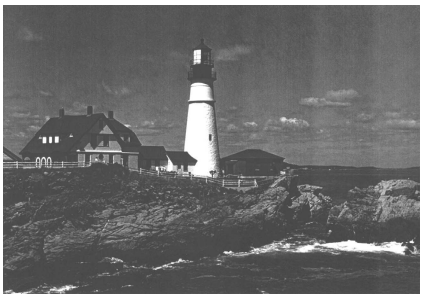
Figure 15 Test image with embedded banding signature

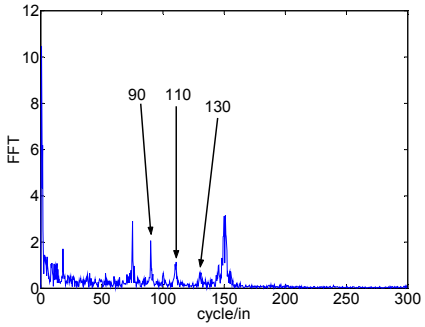

Figure 16 Absorptance spectrum of the test image with embedded signature

VI. Conclusion

We have demonstrated the feasibility to embedded extrinsic signature to an EP printer. Estimation of the embedding banding signal that is below human visual threshold is presented. Higher spatial frequencies provide better trade-off between signal capacity and perception threshold. However, the printer and the subsequent scanner MTF will also limit the range where extrinsic signals can be injected. Since we have ignored the effect of the device MTF, the actual energy of contrast will decrease as embedding frequencies increase. Therefore, the ΔV threshold shown in Fig. 9 is a conservative bound. Advanced embedding and detection algorithms are currently investigating to improve the embedding capacity.

Acknowledgment

We would like to acknowledge the support the National Science Foundation under Grant CCR0219893

References

[1] G. N. Ali, P. J. Chiang, A. K. Mikkilineni, J. P. Allebach, G. T.-C. Chiu and E. J. Delp, "Intrinsic and Extrinsic Signatures for Information Hiding and Secure Printing with Electrophotographic Devices", *IS&T's NIP19: International Conference on Digital Printing Technologies*, p511-515, 2003.

[2] Edward J. Delf, "Is your document safe: An overview of document and print security", in *Proceedings of the IS&T International Conference on Non-Impact Printing*, 2002.

[3] G.Y. Lin, J. Grice, J. Allebach, G. T.-C. Chiu, W. Bradburn, and J. Weaver, "Banding Artifact Reduction in Electrophotographic Printers by Using Pulse Width Modulation", *Journal of Image Science and Technology,* Vol. 46, No. 4, pp.326-337, 2002.

[4] C.-L. Chen, G. T.-C. Chiu, and J. P. Allebach, "Banding Reduction in Electrophotographic Processes Using Human Contrast Sensitivity Function Shaped Photoconductor Velocity Control", *Journal of Image Science and Techology*, Vol. 47, No. 3, pp. 209-223, 2003.

[5] G. N. Ali, a. K. Mikkilineni, P. J. Chiang, J. P. Allebach, G. T.-C. Chiu and E. J. Delp, "Application of Principal Components Analysis and Gaussian Mixture Models to Printer Identification", *IS&T's NIP20: International Conference on Digital Printing Technologies*, p301-305, 2004.

[6] A. K. Mikkilineni, P. J. Chiang, G. N. Ali, G. T.-C. Chiu, J. P. Allebach and E. J. Delp, "Printer Identification Based on Textural Features", *IS&T's NIP20: International Conference on Digital Printing Technologies*, p306-311, 2004.

[7] A. K. Mikkilineni, G. N. Ali, P. J. Chiang, G. T.-C. Chiu, J. P. Allebach and E. J. Delp, „Signature-embedding in Printed Documents for Security and Forensic Applications", *Security, Steganography and Watermarking of Multimedia Contents VI*, p455-466, Jun 22 2004.

[8] A. K. Mikkilineni, O. Arslan, P. J. Chiang, R. M. Kumontoy, J. P. Allebach, G. T.-C. Chiu and E. J. Delp, "Printer Forensic Using SVM Techniques", *IS&T's NIP21: International Conference on Digital Printing Technologies*, p223-226, 2005.

[9] O. Arslan,,R. M. Kumontoy, P.-J. Chiang, A. K. Mikkilineni, J. P. Allebach, G. T.-C. Chiu and E. J. Delp, "Identification of Inkjet Printers for Forensic Applications", *IS&T's NIP21: International Conference on Digital Printing Technologies*, p235-238, 2005.

[10] P. J. Chiang, G. N. Ali, A. K. Mikkilineni, E. J. Delp, J. P. Allebach and G. T.-C. Chiu, "Extrinsic Signatures Embedding Using Exposure Modulation for Information Hiding and Secure Printing in Electrophotography", *IS&T's NIP20: International Conference on Digital Printing Technologies*, p295-300, 2004.

[11] P. J. Chiang, A. K. Mikkilineni, O. Arslan, R. M. Kumontoy, G. T.-C. Chiu, E. J. Delp and J. P. Allebach, "Extrinsic Signatures Embedding in Text Document Using Exposure Modulation for Information Hiding and Secure Printing in Electrophotography", *IS&T's NIP21: International Conference on Digital Printing Technologies*, p231-234, 2005.

[12] L. B. Schein, *Elelcrophotography and Development Phyiscs*, 2nd ed. Morgan Hill, CA: Laplacian Press, 1996.

[13] E. M. Williams, *The Physics and Technology of Xerographic Processes*. New York: Wiley, 1984.

[14] D. Kacker, t. Camis and J. P. Allebach, electrophotographic Process Embedded in Direct Binary Search, *IEEE Trans. On Image Processing*, 11, p234-257, 2002.

[15] A. A. Michelson*, Studies in Optics*, Chicago, Ill.: Univ. Chicago Press, 1927.

[16] F. W. Campbell and D. G. Green, *Optical and Retinal Factors Affecting Visual Resolution*, J. Physiology 181, 576-593, 1965

[17] P. Ahgren and P. Stoica, "High-resolution frequency analysis with small data record", *Electronic Letters*, v36, No. 20, p1745-1747, 28 Sep, 2000.